Medium-dose irradiation impairs long-term hematopoietic stem cell functionality and hematopoietic recovery to cytotoxic stress

Authors

Qinyu Zhang[1,2], Anna Rydström[2,3], Isabel Hidalgo[1,2], Jörg Cammenga[2,3], and Alexandra Rundberg Nilsson[2,3,*]

Affiliations

[1]Medical Faculty, Division of Molecular Hematology, Institution for Laboratory Medicine, Lund University, Sweden.

[2]Medical Faculty, Lund Stem Cell Center, Lund University, Sweden.

[3]Medical Faculty, Division of Molecular Medicine and Gene Therapy, Institution for Laboratory Medicine, Lund University, Sweden.

[*] Corresponding author. Email: alexandra.rundberg_nilsson@med.lu.se

Summary

Irradiation and 5-fluorouracil (5-FU) are widely utilized tools in hematopoietic research to generate myeloablation and assess blood recovery dynamics. A comprehensive understanding of their effects on the hematopoietic system is essential for optimizing therapeutic strategies, refining experimental models to modulate hematotoxicity, and interpreting research outcomes. Despite their widespread application, the long-term hematopoietic impacts of irradiation and 5-FU, particularly on hematopoietic stem cells (HSCs), remain incompletely characterized. In this study, we therefore examined the long-term effects of 2 Gy medium-dose ionizing radiation (MDIR) and 150 mg/kg 5-FU on HSCs and the hematopoietic system's resilience to subsequent cytotoxic stress in

mice. Our findings demonstrate that MDIR, but not 5-FU, induces sustained impairments in HSC function and results in the selective depletion of MHC class II$^-$ HSCs – a subset characterized by high self-renewal potential. Furthermore, MDIR significantly compromised hematopoietic recovery following a subsequent 5-FU challenge, as evidenced by notably reduced platelet and red blood cell (RBC) counts during the critical recovery phase. These findings highlight the distinct and persistent impacts of MDIR and 5-FU on HSCs and hematopoietic function, revealing crucial differences in their mechanisms of action and long-term consequences on the hematopoietic system.

Introduction

Radiation therapy and chemotherapy are foundational pillars in the treatment of cancer, commonly used as standalone interventions or in conjunction with surgery. Additionally, a combination of these modalities, known as chemo-radiation, can be utilized to maximize therapeutic efficacy. Radiation therapy employs high-energy radiation to induce DNA damage, primarily in rapidly proliferating tumor cells, leading to cell death. Chemotherapy, including agents such as 5-fluorouracil (5-FU), is administered systemically and disrupts DNA and RNA synthesis, thereby inhibiting the proliferation of rapidly dividing cells, including cancer cells, and inducing apoptosis. Beyond their clinical applications, both radiation and 5-FU are widely employed in experimental research, particularly for investigating hematopoiesis.

The hematopoietic system, undergoing continuous generation of blood cells, is particularly vulnerable to cytotoxic insults [1]. Hematopoietic stem cells (HSCs), which reside at the apex of the hematopoietic hierarchy, play a crucial role in regenerating the hematopoietic system following injury [2]. Disruptions to HSC function can thus

51 profoundly affect the hematopoietic recovery response under stress. In experimental
52 settings, 5-FU is commonly used to model hematopoietic stress by selectively targeting
53 rapidly dividing cells, such as progenitors and hematopoietic precursor cells. This
54 deletion prompts surviving HSCs to enter the cell cycle and replenish the hematopoietic
55 system [3]. Conversely, lethal and sublethal irradiation has been the standard research
56 strategy to ablate the hematopoietic system prior to transplantation, and to induce DNA
57 damage for studying its biological effects. While both treatments serve as powerful tools
58 in hematopoietic research, they also introduce biological changes that, if not properly
59 understood, can confound experimental results. A thorough understanding of the effects
60 of 5-FU and irradiation on HSCs and hematopoiesis is vital for designing robust
61 experiments, accurately interpreting outcomes, and drawing valid conclusions.
62 Clinically, this knowledge is essential for optimizing cancer treatment regimens and
63 developing strategies to mitigate therapy-induced hematotoxicity.
64
65 In this study, we sought to investigate the long-term hematopoietic effects of 2 Gy
66 medium-dose ionizing radiation (MDIR) and 150 mg/kg 5-FU administration in mice.
67 While 2 Gy is reported to induce DNA damage and 10% lethality in humans [4], 150
68 mg/kg 5-FU is a commonly used dose in murine experimental settings [5, 6]. By
69 examining hematopoietic recovery patterns, including changes in peripheral white blood
70 cells (WBCs), platelets, red blood cells (RBCs), and bone marrow hematopoietic stem
71 and progenitor cell (HSPC) dynamics, we aimed to delineate how these treatments
72 influence hematopoietic resilience to subsequent cytotoxic stress. Our findings offer
73 critical insights into the adaptive capacity of the hematopoietic system and lays the
74 groundwork for optimizing therapeutic regimens.
75

Results

Distinct hematopoietic recovery patterns induced by MDIR and 5-FU

To examine the hematopoietic recovery dynamics following MDIR and 5-FU treatments, wild-type mice were subjected to a) 2 Gy irradiation, b) 150 mg/kg 5-FU, or c) volume-equivalent PBS control (Fig. 1A). Hematopoietic recovery was assessed by monitoring platelet, RBC, and WBC counts in peripheral blood over a three-month period (phase 1). Corroborating prior reports [5, 6], 5-FU treatment resulted in a marked decline in platelet and WBC concentration by day 6 (d6), followed by pronounced rebound peaks by d15, with levels stabilizing thereafter near baseline values (Fig. 1B). Subset analysis of WBCs revealed that eosinophils remained significantly depressed by d15 post 5-FU treatment and did not contribute to the overall WBC rebound peak (Figs. S1 and S2). Additionally, 5-FU caused a substantial reduction in RBCs that was followed by gradual recovery without a rebound peak (Fig. 1B). Conversely, MDIR led to significant reductions in platelet, WBC, and RBC counts, with recovery occurring gradually without any rebound peaks. Together, these results highlight the distinct peripheral blood recovery patterns induced by MDIR and 5-FU treatment, underscoring fundamental differences in how these two cytotoxic agents impact hematopoietic reconstitution.

MDIR results in sustained impairment of HSC functionality

To evaluate the long-term effects of MDIR and 5-FU on primitive hematopoietic populations, we assessed bone marrow HSPC subsets three months post treatments, at phase 1 endpoint. We first characterized alterations in cell counts. MDIR resulted in significant reductions in overall bone marrow cellularity (Fig, 2A) and in specific HSPC subsets, including EPCR^{+} HSCs (herein referred to as HSCs), SLAM HSCs, multipotent progenitors (MPPs), and MPPs biased towards lymphoid (MPP-Ly) and myeloid (MPP-

101 GM) lineages (Fig 2B, gating strategies are provided in Fig. S3A and B). Megakaryocytic
102 and erythroid-primed MPPs (MPP-MkE) were not significantly affected by MDIR.
103 Additionally, MDIR reduced common lymphoid progenitors (CLP), pre-
104 granulocyte/macrophage progenitors (PreGMs), pre-erythroid colony-forming units
105 (PreCFU-Es), and megakaryocytic progenitors (MkPs), while more differentiated
106 myeloid (GMPs) and erythroid (CFU-E/ProEry) precursor populations remained
107 comparable to control levels. In contrast, 5-FU treatment led to a reduction in PreCFU-
108 E precursors but did not significantly impact other analyzed HSPC subsets. To assess the
109 functional consequences on HSCs, we isolated HSCs at the phase 1 endpoint and
110 subjected them to *ex vivo* expansion. While HSCs from the control and 5-FU groups
111 demonstrated similar expansion capacities, HSCs from MDIR-treated mice exhibited a
112 pronounced reduction in *ex vivo* expansion potential (Fig. 2C, Fig. S4A). These findings
113 reveal that MDIR, but not 5-FU, induces sustained reductions across multiple HSPC
114 subsets and leads to a significant long-term impairment in HSC functionality.
115

116 **MDIR impairs the ability to replenish peripheral hematopoietic compartments**
117 **following subsequent 5-FU treatment**

118 To evaluate and compare the long-term impacts of MDIR and 5-FU on hematopoietic
119 recovery ability, all groups were administered 5-FU three months after initial treatment
120 (Fig. 1A; phase 2). While control and 5-FU only groups exhibited similar recovery
121 patterns for RBCs, platelets, and WBCs in peripheral blood during phase 2, notable
122 differences in RBCs and platelets were observed in the irradiated group (Fig. 1B).
123 Irradiated mice experienced a substantially lower RBC nadir on d15 following 5-FU
124 exposure, although all groups exhibited comparable RBC numbers at one month after the
125 exposure (phase 2 endpoint). Additionally, irradiated mice demonstrated persistently

126 lower platelet counts throughout phase 2, with a substantially diminished rebound peak
127 compared to control.
128
129 The impaired platelet recovery observed during phase 2 in irradiated mice may be
130 associated with the reduced MkP numbers observed in the bone marrow at phase 1
131 endpoint (Fig. 2A). Moreover, emergency platelet production can occur directly from
132 $CD41^+$ stem cell-like megakaryocyte-committed progenitors (SL-MkPs) residing within
133 the phenotypical SLAM HSC pool [7]. Further analysis of such cells [7, 8] at phase 1
134 endpoint revealed that irradiated mice, but not the 5-FU group, had considerably
135 decreased SL-MkPs numbers and frequencies (Fig. 2D, Figs. S3B and S4B). Our results
136 demonstrate that MDIR compromises platelet and RBC production during critical
137 recovery phases after subsequent 5-FU treatment, with reductions in MkPs and SL-MkPs
138 likely contributing to the observed deficits in platelet output.
139
140 Finally, bone marrow analysis at phase 2 endpoint revealed no significant differences in
141 cellularity or primitive HSPC populations between the control and 5-FU groups (Fig. 3A-
142 C). However, the irradiated group displayed significantly reduced bone marrow
143 cellularity, accompanied by reductions in HSCs, SLAM-HSCs, MPPs, and MPP-Ly.
144 Notably, the observed reduction in HSC numbers was attributed to a decrease in MHC
145 class II^- HSCs, whereas MHC class II^+ HSC numbers remained unchanged (Fig. 3D and
146 E). To evaluate functional differences between these HSC subtypes, we isolated MHC
147 class II^+ and MHC class II^- HSCs from untreated wild-type mice and subjected them to
148 *ex vivo* expansion. MHC class II^- HSCs exhibited significantly greater self-renew
149 capacity in these cultures (Fig. 3F). Collectively, these findings demonstrate that MDIR
150 impairs the hematopoietic system's resilience to 5-FU-mediated cytotoxic stress, with

151 long-term alterations to both peripheral blood and primitive hematopoietic bone marrow
152 compartments. The preferential loss of MHC class II$^-$ HSCs, which exhibit enhanced self-
153 renewal, highlights a critical and lasting impairment of hematopoietic regenerative
154 capacity following MDIR.
155
156 **Discussion**
157 Our study advances the understanding of the differential effects of MDIR and 5-FU on
158 hematopoietic recovery, with a focus on the long-term consequences for HSPCs and
159 subsequent stress responses. Through a comparative analysis of these common
160 hematopoietic stressors, we identified unique recovery patterns and cellular responses
161 that reveal distinct mechanisms driving hematopoietic reconstitution.
162
163 Hematopoietic recovery following 5-FU treatment featured transient reductions in
164 peripheral blood platelet and WBC counts, followed by robust rebound peaks. RBC
165 counts similarly declined, reaching its nadir concurrently with WBCs and platelets, but
166 displayed delayed recovery without an overshoot. These patterns, consistent with prior
167 studies [5, 6], suggest that 5-FU's selective targeting of proliferating cells is followed by
168 compensatory mechanisms to restore depleted populations. By employing control groups
169 at each time point, we enhanced the accuracy of our findings compared to previous
170 studies that compared the recovery levels against pre-treatment levels [5, 6], providing a
171 clearer picture of hematopoietic recovery dynamics post-5-FU treatment. Moreover, our
172 study uniquely characterizes WBC subset-specific responses, showing that eosinophils,
173 unlike other subsets, fail to exhibit a compensatory overshoot. This subset-specific
174 variability implies distinct regulatory mechanisms underlying WBC recovery and
175 suggests that certain immune cell types may be more vulnerable to hematopoietic insults.

176

177 Prior research has shown that, unlike in the peripheral blood, 5-FU causes a transient
178 reduction in bone marrow WBCs without a subsequent recovery peak [6, 9]. Moreover,
179 colony-forming unit (CFU) assays have demonstrated an initial decline in CFU
180 frequencies after 5-FU treatment, followed by an overshoot [6, 9]. However, since CFUs
181 are primarily derived from hematopoietic progenitor cells, rather than true HSCs [10-13],
182 CFU assays cannot reliably evaluate HSC functionality. Additionally, changes in CFU
183 frequencies or HSC proportions may not reflect actual HSC population dynamics, as
184 shifts in one cell type can impact the proportions of others [14]. Our results demonstrate
185 that 5-FU does not compromise the long-term integrity or function of HSCs, with $EPCR^+$
186 HSCs maintaining stable numbers and functionality three months post-5-FU exposure.
187 Furthermore, exposure to a prior 5-FU dose did not modify hematopoietic recovery in
188 response to a second 5-FU treatment, underscoring the transient impact of 5-FU on
189 progenitor cells without affecting HSCs' capacity for sustained hematopoietic recovery.

190

191 MDIR-induced hematopoietic suppression proved to be more persistent. MDIR triggered
192 reductions in peripheral blood platelets, WBCs, and RBCs without rebound peaks,
193 corroborating previous studies demonstrating the inability of MDIR to elicit a rapid
194 compensatory response, unlike 5-FU [5, 6, 9, 15]. Previous studies have documented that
195 MDIR results in short-term declines in bone marrow cellularity, CFUs, and SLAM HSCs
196 [5, 6, 9, 15, 16], and long-term reductions in SLAM HSC frequencies [17]. We showed
197 that MDIR led to lasting reductions in bone marrow cellularity and key HSPC subsets,
198 including the more purified $EPCR^+$ HSCs, which additionally exhibited impaired self-
199 renewal capacity on a per cell basis. These enduring impacts, as opposed to the transient
200 effects of 5-FU, indicate that radiation imposes more profound disruptions on the

201 hematopoietic system, affecting not only cellularity but also HSC functionality and
202 regenerative capacity.
203
204 Importantly, we also show that MDIR affects the hematopoietic recovery upon exposure
205 to a subsequent 5-FU dose administered three months post MDIR exposure. The
206 significantly lower platelet and RBC levels observed during the recovery phase following
207 5-FU in these mice, particularly the reduced platelet recovery peak, suggest a
208 compromised emergency hematopoiesis response. This persistent impairment may arise
209 from the sustained reduction in specific progenitor cells, such as MkPs, or platelet-biased
210 $CD41^+$ SL-MkPs that we observed in irradiated mice at the time of the 5-FU exposure,
211 supporting previous studies indicating SL-MkPs role in emergency hematopoiesis [7].
212 Our data also reveal a novel vulnerability of MHC class II^- HSCs to MDIR, with this
213 subpopulation showing significant reductions one month after 5-FU administration to the
214 MDIR group, at the end of phase 2 – a finding not observed in the 5-FU only group.
215 Given that MHC class II^- HSCs exhibited enhanced self-renewal capacity, their depletion
216 may particularly impair hematopoietic recovery, underscoring the differential impacts of
217 MDIR on distinct HSC subsets. Notably, HSCs expressing low levels of MHC class II
218 also exhibit increased platelet potential [18], potentially further contributing to the
219 decreased platelet output observed during phase 2 in the MDIR group. These findings
220 have important implications for experimental models and therapeutic strategies that seek
221 to minimize long-term hematotoxicity while enhancing HSC recovery post-radiation
222 exposure.
223
224 In conclusion, our findings have significant implications for HSC research, where both
225 5-FU and irradiation are commonly used to model hematopoietic stress and investigate

226 HSC biology. We demonstrate that MDIR and 5-FU elicit distinct effects on HSC
227 populations and hematopoietic recovery, with MDIR inducing more enduring
228 impairment in HSC functionality. The differential responses of HSC subpopulations,
229 including the selective vulnerability of MHC class II$^-$ HSCs to MDIR, highlight the
230 complexity of hematopoietic responses to stress. These results emphasize the need for
231 nuanced experimental design and interpretation, particularly in studies exploring HSC
232 heterogeneity and regeneration. Clinically, the findings underscore the importance of
233 careful consideration in therapeutic regimens involving radiation, where the potential for
234 long-term hematologic complications, such as anemia or thrombocytopenia, necessitates
235 strategies to mitigate hematopoietic impairment. Enhancing emergency hematopoiesis in
236 irradiated patients could improve outcomes in clinical contexts, underscoring the
237 relevance of our findings for both research and patient care.
238
239 **Material and methods**
240 **Mice and treatments**. Female C57BL/6N mice aged 12 to 13 weeks were used
241 throughout the study. 2 Gy MDIR was delivered via exposure to a Cesium-137 source.
242 5-FU was administered intraperitoneally (i.p.) at a dose of 150 mg/kg body weight.
243 Control mice received volume-equivalent doses of PBS via i.p. injections. Mice were
244 housed at the Lund University Biomedical Center vivarium, with all procedures
245 performed in strict accordance with ethical permits granted by the Malmö/Lund Animal
246 Ethics Board (permit number 18055/2020).
247
248 **Peripheral blood cell monitoring and bone marrow cell analysis.** Peripheral blood
249 and bone marrow were isolated and assessed as previously described [19, 20]. Briefly,
250 the blood was collected from the tail vein into EDTA-coated collection tubes and

251 analyzed using a Sysmex Hemato Analyzer XN-350™ for cellularity counts. Blood
252 samples were incubated at 37° for 25 minutes in FACS buffer (PBS containing 2% fetal
253 bovine serum and 0.2 mM EDTA) supplemented with 1% Dextran. The WBC-rich
254 upper phase was collected, and RBCs were lysed using RBC lysis solution
255 (STEMCELL Technologies Inc.) at room-temperature for 3 minutes. Cells were stained
256 with conjugated antibodies targeting CD4, CD8, NK1.1, CD19, CD11b, Gr-1, and
257 CD45.2. Bone marrow cells were harvested from crushed tibias, femurs and iliac bones.
258 Lineage depletion (B220, CD3, Gr-1, and Ter119) was performed prior to sorting using
259 MACS magnetic microbead kits (Miltenyi Biotec) according to the manufacturer's
260 instructions. Cells were stained with conjugated antibodies for B220, CD3, Gr-1,
261 Ter119, cKit, Sca-1, CD48, CD150, EPCR, FLT3, IL-7Ra, CD105, CD41, CD16/32,
262 and MHC class II. Streptavidin-BV605 was used for biotin identification, and cell
263 viability was assessed with propidium iodide (1 μg/ml; Molecular Probes). Flow
264 cytometry analysis and cell sorting were performed on a Becton Dickinson (BD) LSR
265 Fortessa X-20 and a BD Aria III. Cell type isolation markers and flow cytometry gating
266 strategies are provided in the Supplementary materials.
267
268 ***Ex vivo* HSC expansion cultures**. HSCs were expanded *ex vivo* following the protocol
269 described in [21]. Briefly, 50 EPCR$^+$ HSCs were sorted onto fibronectin-coated cell
270 culture dishes containing F12 medium supplemented with 1% Insulin-transferring-
271 selenium-ethanolamine, 1% penicillin/streptomycin/glutamine, 10 mM HEPES, 0.1%
272 PVA (Sigma), 10 ng/mL stem cell factor and 100 ng/mL thrombopoietin. Cultures were
273 maintained for 13 to14 days. Cellularity was quantified using a TC20 automated cell
274 counter (Bio-Rad). Relative cell counts were assessed using flow cytometry analysis on
275 a BD LSR Fortessa X-20, employing time-, volume, and speed-standardized settings.

Acknowledgments

We extend our gratitude to Dr. David Bryder for his insightful feedback and valuable support throughout the course of this study. We also thank the staff at the Lund University vivarium and flow cytometry core facility for their diligent work.

Funding: ARN was supported by grants from Lindhés advokatbyrå, Gunnar Nilssons Cancerstiftelse, Åke Wibergs stiftelse, and Magnus Bergvalls stiftelse. JC was supported by grants from The Swedish Cancer Society, and The Swedish Childhood Cancer Fund.

Author contributions:

Conceptualization: ARN, JC

Methodology and investigation: ARN, AR, IH, QZ

Visualization: ARN

Supervision: ARN, JC

Writing: ARN

Competing interests: The authors declare no competing interests.

Data and materials availability: All data needed to evaluate the conclusions in the paper are present in the paper and/or the Supplementary Materials. Key resources are listed in Table S1.

Declaration of generative AI and AI-assisted technologies in the writing process: During the preparation of this work the author(s) used ChatGPT in order to improve language and readability. After using this tool/service, the author(s) reviewed and edited the content as needed and take(s) full responsibility for the content of the publication.

References

1. Henry, E. and M.L. Arcangeli, *How Hematopoietic Stem Cells Respond to Irradiation: Similarities and Differences between Low and High Doses of Ionizing Radiations.* Exp Hematol, 2021. **94**: p. 11-19.
2. Pietras, E.M., et al., *Functionally Distinct Subsets of Lineage-Biased Multipotent Progenitors Control Blood Production in Normal and Regenerative Conditions.* Cell Stem Cell, 2015. **17**(1): p. 35-46.
3. Randall, T.D. and I.L. Weissman, *Phenotypic and functional changes induced at the clonal level in hematopoietic stem cells after 5-fluorouracil treatment.* Blood, 1997. **89**(10): p. 3596-606.
4. Squillaro, T., et al., *Concise Review: The Effect of Low-Dose Ionizing Radiation on Stem Cell Biology: A Contribution to Radiation Risk.* Stem Cells, 2018. **36**(8): p. 1146-1153.
5. Li, X. and W.B. Slayton, *Molecular mechanisms of platelet and stem cell rebound after 5-fluorouracil treatment.* Exp Hematol, 2013. **41**(7): p. 635-645 e3.
6. Kojima, E. and A. Tsuboi, *Effects of 5-fluorouracil on hematopoietic stem cells in normal and irradiated mice.* J Radiat Res, 1992. **33**(3): p. 218-26.

323 7. Haas, S., et al., *Inflammation-Induced Emergency Megakaryopoiesis Driven by*
324 *Hematopoietic Stem Cell-like Megakaryocyte Progenitors.* Cell Stem Cell, 2015. **17**(4):
325 p. 422-34.
326 8. Pronk, C.J., et al., *Elucidation of the phenotypic, functional, and molecular topography*
327 *of a myeloerythroid progenitor cell hierarchy.* Cell Stem Cell, 2007. **1**(4): p. 428-42.
328 9. Nielsen, O.S., H. von der Maase, and J. Overgaard, *Effect of combined 5-fluorouracil*
329 *and radiation on murine hematopoietic tissue.* Radiother Oncol, 1988. **13**(2): p. 145-
330 52.
331 10. Hodgson, G.S. and T.R. Bradley, *Properties of haematopoietic stem cells surviving 5-*
332 *fluorouracil treatment: evidence for a pre-CFU-S cell?* Nature, 1979. **281**(5730): p.
333 381-2.
334 11. Van Zant, G., *Studies of hematopoietic stem cells spared by 5-fluorouracil.* J Exp Med,
335 1984. **159**(3): p. 679-90.
336 12. Dick, J.E., et al., *Introduction of a selectable gene into primitive stem cells capable of*
337 *long-term reconstitution of the hemopoietic system of W/Wv mice.* Cell, 1985. **42**(1): p.
338 71-9.
339 13. Schofield, R., *The relationship between the spleen colony-forming cell and the*
340 *haemopoietic stem cell.* Blood Cells, 1978. **4**(1-2): p. 7-25.
341 14. Rundberg Nilsson, A., C.J. Pronk, and D. Bryder, *Probing hematopoietic stem cell*
342 *function using serial transplantation: Seeding characteristics and the impact of stem*
343 *cell purification.* Exp Hematol, 2015. **43**(9): p. 812-7 e1.
344 15. Kojima, E. and A. Tsuboi, *Protection of survival and hematopoiesis in irradiated mice*
345 *by 5-fluorouracil.* Jpn J Cancer Res, 1992. **83**(7): p. 783-8.
346 16. Mohrin, M., et al., *Hematopoietic stem cell quiescence promotes error-prone DNA*
347 *repair and mutagenesis.* Cell Stem Cell, 2010. **7**(2): p. 174-85.

348 17. Rodrigues-Moreira, S., et al., *Low-Dose Irradiation Promotes Persistent Oxidative*
349 *Stress and Decreases Self-Renewal in Hematopoietic Stem Cells.* Cell Rep, 2017.
350 **20**(13): p. 3199-3211.
351 18. Li, J., et al., *STAT1 is essential for HSC function and maintains MHCIIhi stem cells that*
352 *resist myeloablation and neoplastic expansion.* Blood, 2022. **140**(14): p. 1592-1606.
353 19. Rundberg Nilsson, A.J.S., et al., *IRF1 regulates self-renewal and stress responsiveness*
354 *to support hematopoietic stem cell maintenance.* Sci Adv, 2023. **9**(43): p. eadg5391.
355 20. Rundberg Nilsson, A., et al., *Temporal dynamics of TNF-mediated changes in*
356 *hematopoietic stem cell function and recovery.* iScience, 2023. **26**(4): p. 106341.
357 21. Zhang, Q., et al., *Ex vivo expansion potential of murine hematopoietic stem cells is a*
358 *rare property only partially predicted by phenotype.* Elife, 2024. **12**.
359
360

361 **Figures**

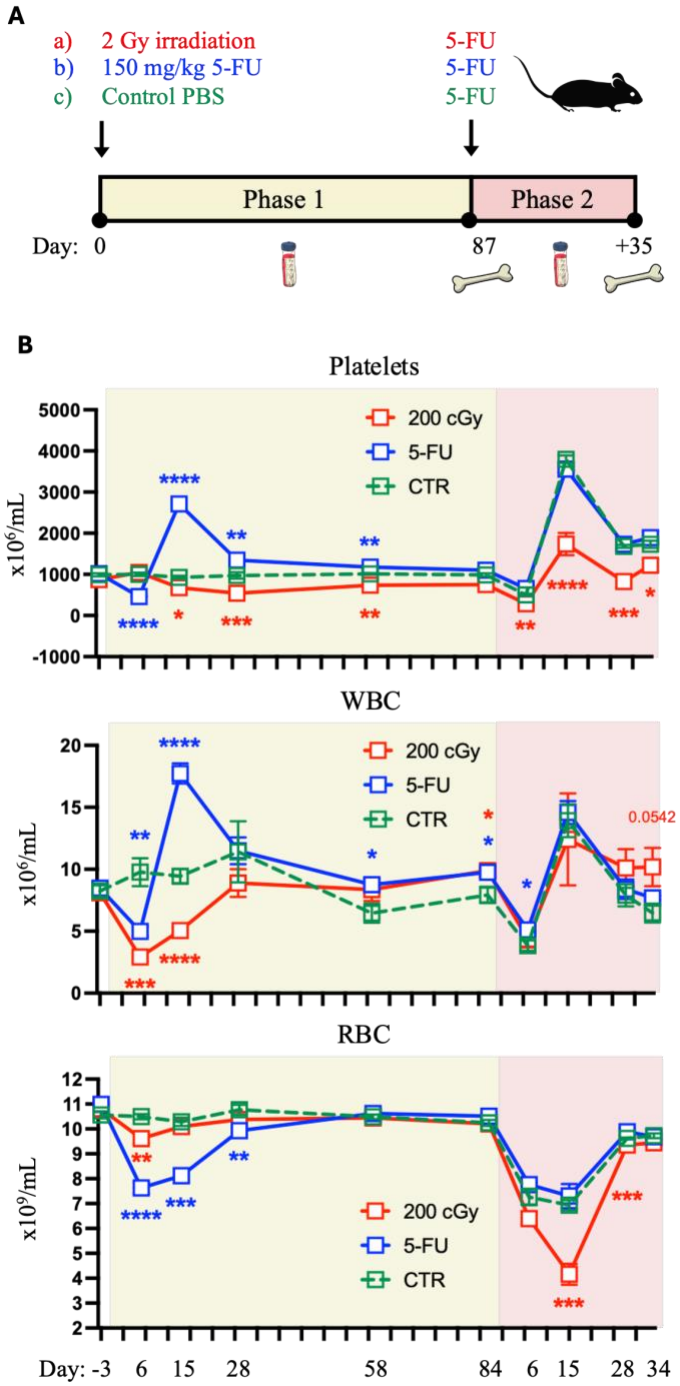

362 **Fig. 1. MDIR and 5-FU induce distinct peripheral blood recovery dynamics. (A)**
363 Experimental design. 13-week-old female C57BL/6N mice were divided into three
364 groups: medium-dose irradiation (2 Gy), 150 mg/kg 5-FU, or control (phosphate-
365 buffered saline, PBS). Mice were monitored for hematopoietic recovery over a 3-month
366 period (phase 1). Following this, all groups were administered 150 mg/kg 5-FU and were

observed for an additional month (phase 2). Peripheral blood counts were assessed at multiple timepoints throughout the study, with bone marrow analyses performed at phase endpoints. **(B)** Time course of peripheral blood platelet, WBC, and RBC concentrations. Sample sizes: control (n=5), 2 Gy (n=5 during phase 1, days -3 to 58; n=4 during the remainder), and 5-FU (n=5). Statistical significance is indicated for comparisons between treated groups and control. Error bars represent mean ± SEM. *$p < 0.05$, **$p < 0.01$, ***$p < 0.001$, ****$p < 0.0001$.

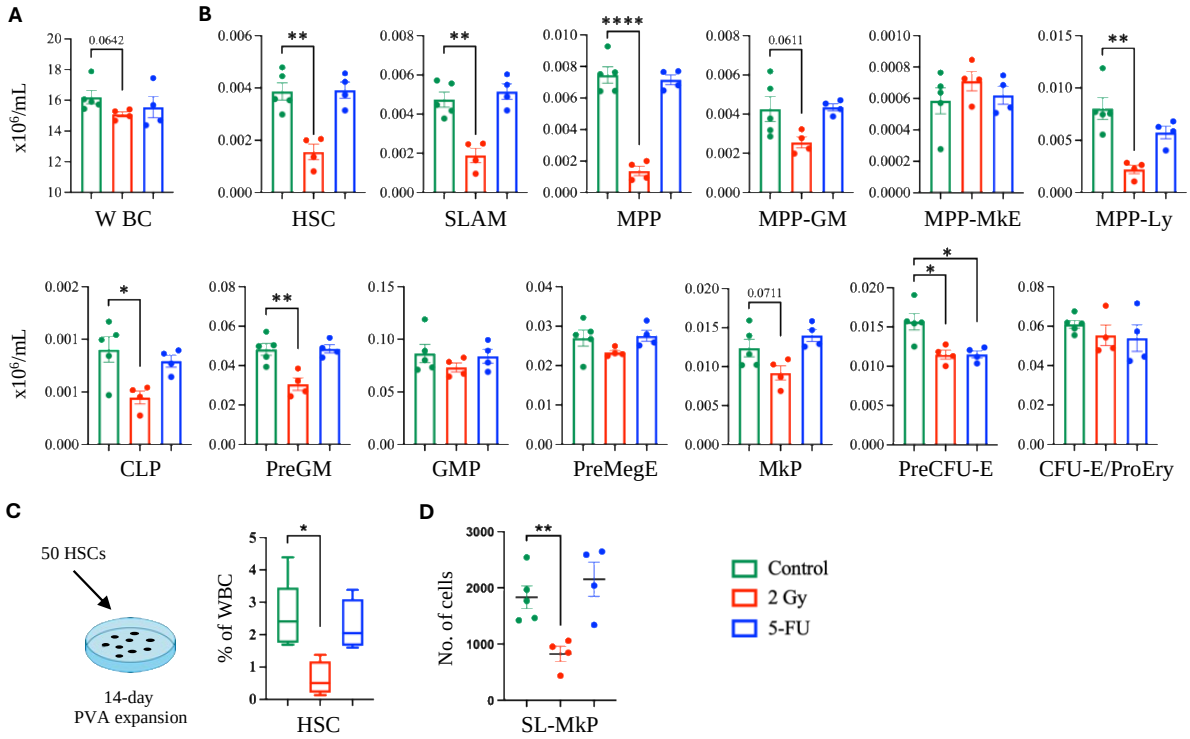

Fig. 2. MDIR results in sustained impairments in the HSC pool. (A) Bone marrow WBC cellularity and **(B)** HSPC at the end of phase 1. **(C)** *Ex vivo* HSC expansion assay design (left) and frequency of HSCs after 14 days of culture (right). **(D)** Number of SL-MkPs in the bone marrow at the phase 1 endpoint. Control n=5, 2 Gy n=4, 5-FU n=4. Error bars represent mean ± SEM for panels A, B and D, and Min/Max for panel C. Statistical significance is indicated for comparisons between treated groups and control. *$p < 0.05$, **$p < 0.01$, ***$p < 0.001$, ****$p < 0.0001$.

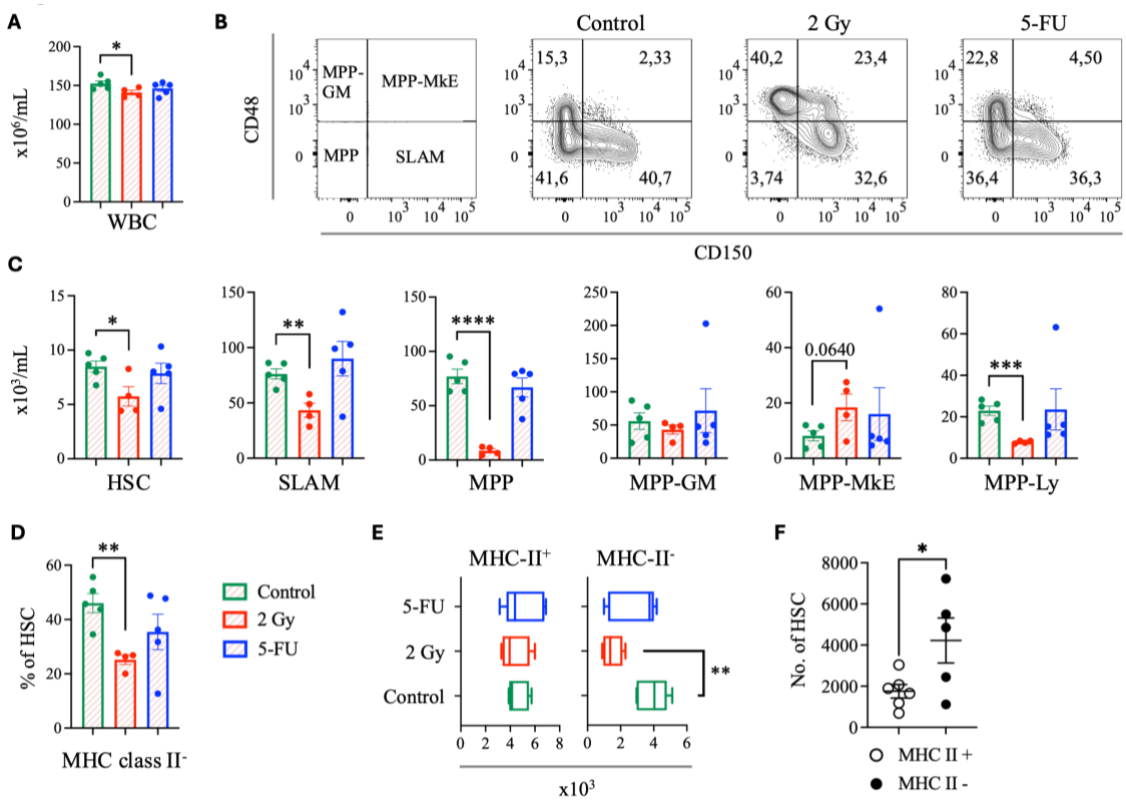

Fig. 3. MHC class II-negative HSCs are functionally superior and are selectively depleted by MDIR. (A) Bone marrow WBC cellularity, **(B)** representative flow cytometry plots showing LSK populations, and **(C)** HSPC counts at the phase 2 endpoint. **(D)** Frequency of MHC class II^{-} within HSCs, and **(E)** quantification of MHC class II positive and negative HSC populations at the phase 2 endpoint. Control n=5, 2 Gy n=4, 5-FU n=5. **(F)** Number of HSCs after 13 days of *ex vivo* expansion from either MHC class II positive or negative HSCs. Control n=5, 2 Gy n=4, 5-FU n=4. Significance asterisks indicate differences in treatment groups compared to the control group. Error bars represent mean ± SEM (A, C, D and F), or Min/Max (E). *$p < 0.05$, **$p < 0.01$, ***$p < 0.001$, ****$p < 0.0001$.

Supplementary Figures

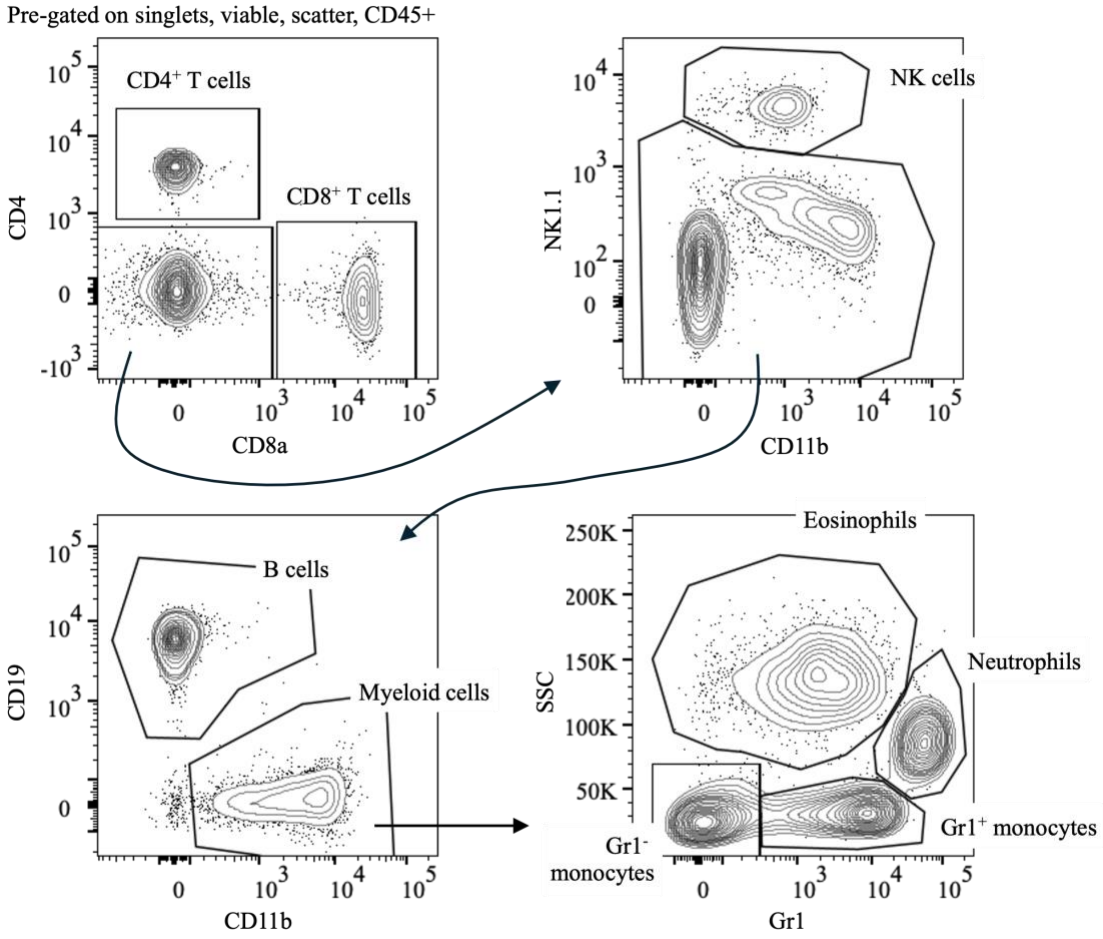

Fig. S1. Gating strategy for peripheral blood WBC subsets. Cells were pre-gated on singlet discrimination, viability, size and complexity (FSC-A/SSC-A profiles), and $CD45^+$ expression. The following subsets were identified: $CD4^+$ T cells = $CD4^+CD8^-$, $CD8^+$ T cells = $CD8^+CD4^-$, NK cells = $NK1.1^+CD4^-CD8^-$, B cells = $CD19^+NK1.1^-CD4^-CD8^-$, Myeloid cells = $CD11b^+CD19^+NK1.1^-CD4^-CD8^-$, Eosinophils = $SSC^{high}Gr1^{low/med}CD11b^+CD19^+NK1.1^-CD4^-CD8^-$, neutrophils = $SSC^{med}Gr1^{high}CD11b^+CD19^+NK1.1^-CD4^-CD8^-$, $Gr1^+$ monocytes = $SSC^{low}Gr1^+CD11b^+CD19^+NK1.1^-CD4^-CD8^-$, $Gr1^-$ monocytes = $SSC^{low}Gr1^-CD11b^+CD19^+NK1.1^-CD4^-CD8^-$.

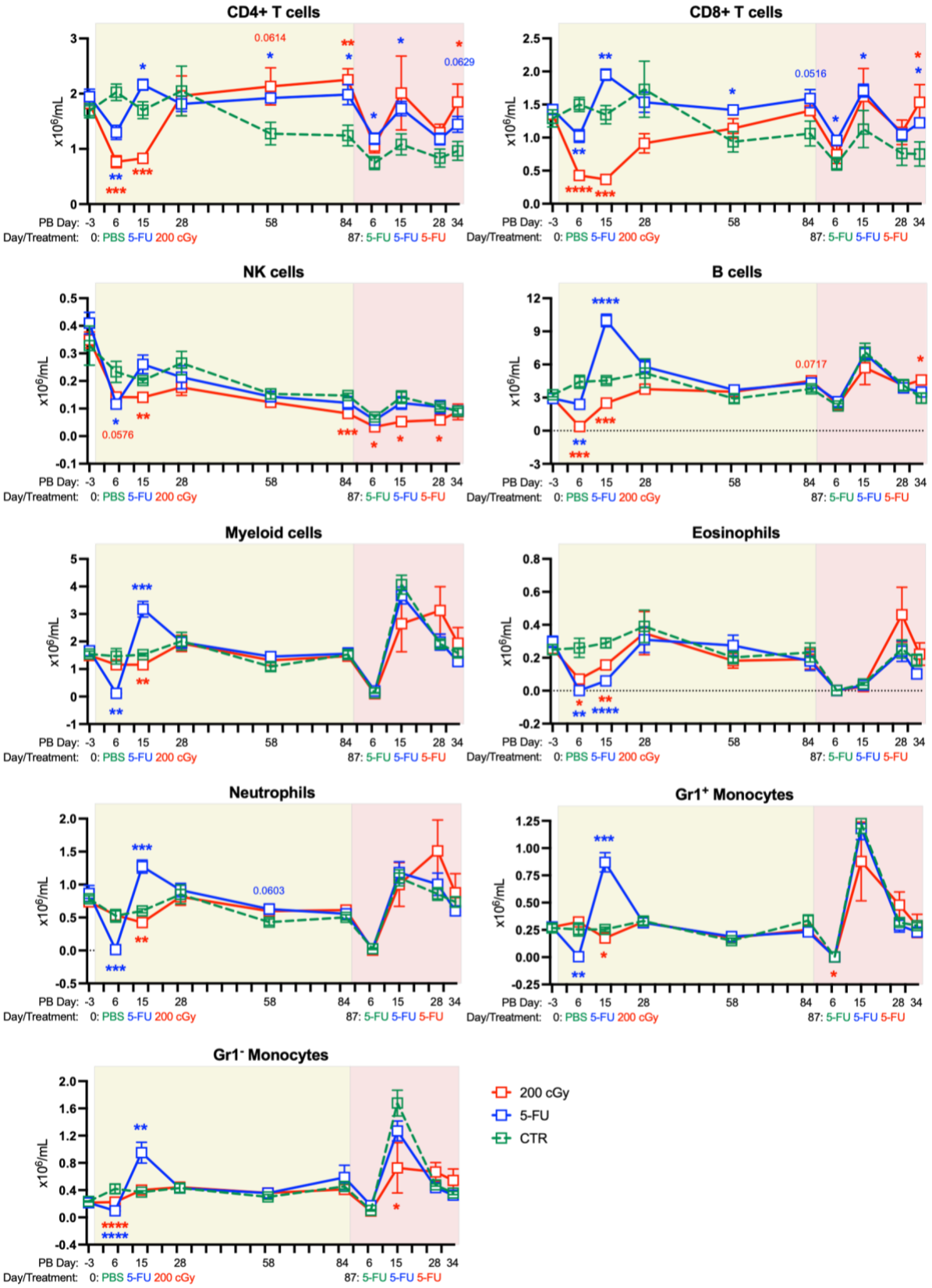

Fig. S2. Time course of peripheral blood WBC subset concentrations. Control (n=5), 2 Gy (n=5 during phase 1, days -3 to 58; n=4 during the remainder), and 5-FU (n=5). Statistical

412 significance is indicated for comparisons between treated groups and control. Error bars

413 represent mean ± SEM. *$p < 0.05$, **$p < 0.01$, ***$p < 0.001$, ****$p < 0.0001$.

414

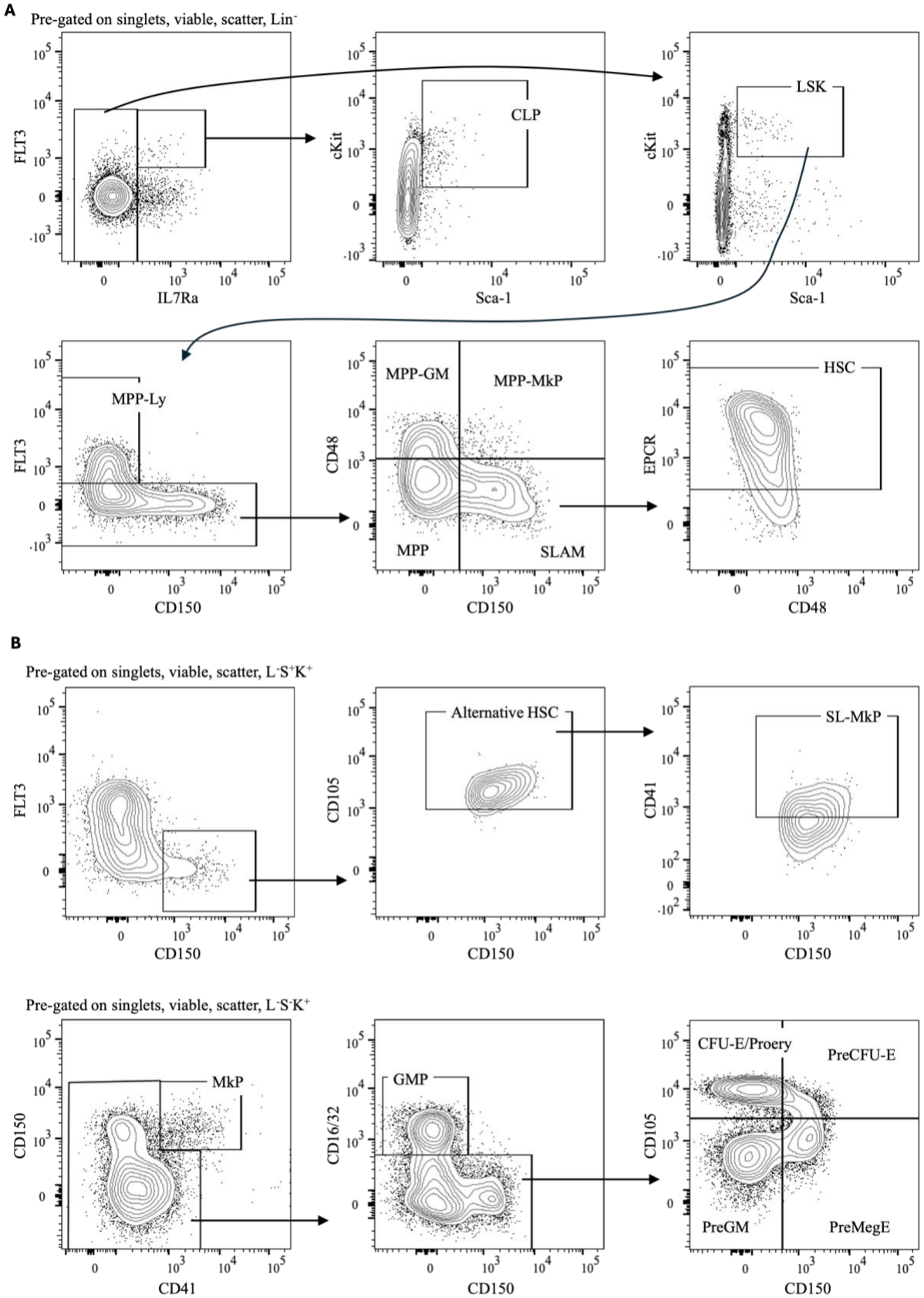

415

416 **Fig. S3. Gating strategy for bone marrow HSPC subsets. (A)** Cells were pre-gated on singlet

417 discrimination, viability, size and complexity (FSC-A/SSC-A profiles), and lineage

418 (B220, CD3, Gr1 and Ter119) negativity. The following subsets were identified: CLP =
419 $FLT3^{+}IL7Ra^{+}Sca\text{-}1^{med}cKit^{med}$, MPP-Ly = $FLT3^{+}CD150^{-}IL7Ra^{-}Sca\text{-}1^{+}cKit^{+}$, MPP-MkP =
420 $CD48^{+}CD150^{+}FLT3^{-}IL7Ra^{-}Sca\text{-}1^{+}cKit^{+}$, MPP-GM = $CD48^{+}CD150^{-}FLT3^{-}IL7Ra^{-}Sca\text{-}$
421 $1^{+}cKit^{+}$, MPP = $CD48^{-}CD150^{-}FLT3^{-}IL7Ra^{-}Sca\text{-}1^{+}cKit^{+}$, SLAM = $CD48^{-}CD150^{+}FLT3^{-}$
422 $IL7Ra^{-}Sca\text{-}1^{+}cKit^{+}$, HSC = $EPCR^{+}CD48^{-}CD150^{+}FLT3^{-}IL7Ra^{-}Sca\text{-}1^{+}cKit^{+}$. **(B)** Cells
423 were pre-gated on singlet discrimination, viability, size and complexity (FSC-A/SSC-A
424 profiles), as well as lineage (B220, CD3, Gr1 and Ter119) negativity, $Sca\text{-}1^{-}$ and $cKit^{+}$
425 ($L^{-}S^{-}K^{+}$; upper panel) or $L^{-}S^{+}K^{+}$ (LSK; lower panel). The following subsets were
426 identified: SL-MkP = $L^{-}S^{+}K^{+}CD150^{-}CD105^{+}FLT3^{-}CD41^{+}$, MkP = $L^{-}S^{-}$
427 $K^{+}CD150^{+}CD41^{+}$, GMP = $L^{-}S^{-}K^{+}CD150^{-}CD41^{-}CD16/32^{+}$, PreGM = $L^{-}S^{-}K^{+}CD150^{-}$
428 $CD105^{-}CD41^{-}CD16/32^{-}$, PreMegE = $L^{-}S^{-}K^{+}CD150^{+}CD105^{-}CD41^{-}CD16/32^{-}$, PreCFU-E
429 = $L^{-}S^{-}K^{+}CD150^{+}CD105^{+}CD41^{-}CD16/32^{-}$, and CFU-E/ProEry = $L^{-}S^{-}K^{+}CD150^{-}$
430 $CD105^{+}CD41^{-}CD16/32^{-}$.
431

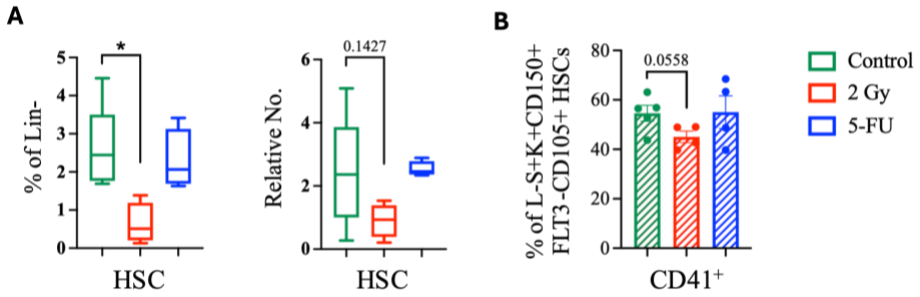

Fig. S4. The long-term impact of MDIR and 5-FU on HSCs. (A) HSC frequency within the Lin^- compartment (left), and relative cell numbers (right) after 14 days of *ex vivo* expansion culture from HSCs isolated at phase 1 endpoint. **(B)** Frequency of $CD41^+$ cells (SL-MkPs) within the alternative $L^-S^+K^+FLT3^-CD150^+CD105^+$ HSC population [8] at the end of phase 1. Control n=5, 2 Gy n=4, 5-FU n=4. Error bars represent mean ±Min/Max for panel A, and ±SEM for panel B. Statistical significance is indicated for comparisons between treated groups and control. *$p < 0.05$, **$p < 0.01$, ***$p < 0.001$, ****$p < 0.0001$.

Supplementary tables

Table S1. Key resource table

REAGENT or RESOURCE	SOURCE	IDENTIFIER
Antibodies		
Biotin anti-mouse/human CD45R/B220 (RA3-6B2)	BioLegend	Cat: 103204
Biotin anti-mouse CD3e (145-2C11)	BD Pharmingen	Cat: 100404
Biotin anti-mouse Ly-6G/Ly6C (Gr-1) (RB6-8C5)	BioLegend	Cat: 108404
Biotin anti-mouse TER-119/Erythroid Cells (TER-119)	BioLegend	Cat: 116204
PE/Cy5 anti-mouse/human CD45R/B220 (RA3-6B2)	BioLegend	Cat: 103209
PE/Cy5 anti-mouse Ly-6G/Ly6C (Gr-1) (RB6-8C5)	SONY	Part: 1142050
PE/Cy5 anti-mouse TER-119/Erythroid Cells (TER-119)	BioLegend	Cat: 116209
PE/Cy5 anti-mouse CD3ε (145-211)	BioLegend	Cat: 100309
APC/Cy7 anti-mouse CD4 (RM4-5)	BioLegend	Cat: 100526
PE/Cy5 anti-mouse CD8a (53-6.7)	BioLegend	Cat: 100709
APC anti-mouse human CD11b (M1/70)	BioLegend	Cat: 101212
PE/Cy7 anti-mouse CD19 (6D5)	BioLegend	Cat: 115520
FITC anti-mouse CD45.2 (104)	BioLegend	Cat: 109806
APC-eFluor780 anti-mouse CD117 (c-Kit) (2B8)	Invitrogen	Ref: 47-1171-82
Pacific Blue anti-mouse Ly-6A/E (Sca-1) (E13-16.7)	BioLegend	Cat: 122520
Alexa Fluor 700 anti-mouse CD48 (HM48-1)	BioLegend	Cat: 103426
PE/Cy7 anti-mouse CD48 (HM48-1)	BioLegend	Cat: 103424
PE/Cy7 anti-mouse CD150 (TC15-12F12.2)	BioLegend	Cat: 115914
APC anti-mouse CD150 (TC15-12F12.2)	BioLegend	Cat: 115910
PE anti-mouse CD135 (FLT3) (A2F10))	BioLegend	Cat: 135306
PE/Cy7 anti-mouse CD105 (MJ7/18)	BioLegend	Cat: 120410
FITC anti-mouse CD41 (MWReg30)	BioLegend	Cat: 133904
Alexa Fluor 700 anti-mouse CD16/32 (93)	Invitrogen	Ref: 56-0161-82
Brilliant Violet 605 Streptavidin	BioLegend	Cat: 405229

Chemicals, peptides, medium, and recombinant proteins		
Animal-free recombinant murine TPO	PeproTech	Cat: AF-31514
Animal-free recombinant murine SCF	PeproTech	Cat: AF-20503
Propidium Iodide	Molecular Probes	Cat: P3566
GibcoTM Ham's F-12 Nutrient Mix	Gibco	Cat: 11765054
GibcoTM Insulin-Transferrin-Selenium-Ethanolamine (ITS - X)	Gibco	Cat: 51500056
GibcoTM HEPES (1M)	Gibco	Cat: 15630080
Polyvinyl alcohol (PVA)	Sigma	Cat: 363081
GibcoTM Penicillin-Streptomycin-Glutamine (100X)	Gibco	Cat: 10378016
Fibronectin	Sigma	Cat: F0895
Dulbecco's phosphate-buffered saline (DPBS)	Sigma	Cat: 14190169
Experimental models: Organisms/strains		
Mouse: C57Bl/6N	Taconic Biosciences A/S	
Software and algorithms		
FlowJo	BD, Treestar	v. 10
GraphPad Prism	Dotmatics	v. 9